FERMILAB-PUB-76-147-E

EFI 76-47

Production of ^{24}Na and ^{18}F from ^{27}Al with 400-GeV protons*

S. K. Chang and Nathan Sugarman
The Enrico Fermi Institute, The University of Chicago
Chicago, Illinois 60637

(Received)

The recoil properties of ^{24}Na and ^{18}F from the interaction of ^{27}Al with 400 GeV protons were measured. The results showed little change in the production mode of these simple spallation reactions at 400 GeV from lower incident proton energies. No evidence was seen for inelasticity in the primary proton-nucleus interaction.

The cross section for ^{18}F production was found to be 5.9 ± 0.2 mb, 74% that of ^{24}Na.

[NUCLEAR REACTIONS $^{27}Al(p,x)^{24}Na$, ^{18}F. T_p=400 GeV; measured thick target recoil properties and σ for ^{18}F; production mechanism discussed.]

Submitted to PHYSICAL REVIEW C

I. INTRODUCTION

The production of nuclei from the interaction of high energy protons with complex nuclei is usually described by a two-step model,[1] a fast intranuclear cascade process followed by a slower deexcitation step. This model works well for most nuclear reactions in the 100-500 MeV[2,3] region, but has difficulty explaining the production of products formed from highly excited heavy nuclei at proton energies greater than 3 GeV.[4] Since the origin of the difficulty is not clear, it was thought worthwhile to reexamine a simple spallation reaction, $^{27}Al(p,3pn)^{24}Na$, at energies $\gtrsim$ 3 GeV to see how well understood its production mechanism is. The kinematics of the ^{24}Na reaction have been studied using the recoil technique at proton energies from 30 to 90 MeV by Hintz,[5] from 60 to 340 MeV by Fung and Perlman,[6] from 0.5 to 28 GeV by Poskanzer et al.,[7] and from 3 to 300 GeV by Steinberg and Winsberg.[8] At proton energies lower than 80 MeV, the reaction proceeds through the formation of a compound nucleus followed by the evaporation of nucleons. At higher incident energy, only partial transfer of the linear momentum takes place. In general, the ratio of forward-to-backward recoils decreases with increasing proton energy but the range of the recoils in the frame of the struck target nucleus remains constant. The former is a consequence of the cascade process, the latter of the deexcitation process. These two steps will be examined separately in the analysis of the results.

In the course of this work, the production cross section and recoil properties of ^{18}F formed from ^{27}Al by bombardment with 400-GeV protons were also measured.

II. EXPERIMENTAL

The target assemblies used in these experiments are shown in Fig. 1 (Fig. 1a and 1b). A high purity Al foil, 6.8 mg/cm^2 in thickness, was sandwiched between several foils of Mylar, 17 mg/cm^2 thick. The foils were cemented on the edges and were kept under vacuum before bombardment. The irradiations were performed in the Meson Laboratory area of the Fermi National Accelerator Laboratory. The duration of bombardment varied from 10 min to 1 hr, the integrated beam from 5×10^{13} to 5×10^{14} protons.

After bombardment, an area of 3 cm^2 surrounding the beam spot was punched out and the radioactivity of ^{24}Na and ^{18}F in each foil was assayed. The ^{24}Na activity was determined by methane-flow gas proportional beta counters of known geometry and the 511-Kev positron annihilation γ rays of the ^{18}F activity by two NaI crystals in coincidence. The counters were calibrated with standards of known disintegration rate. The data from the proportional counters showed the dominance of the 15h ^{24}Na activity from one day after the bombardment until a week later. There was also a long-lived component probably from the decay of ^{22}Na. The NaI coincidence

decay curves, after allowing for the decay of 20m ^{11}C, had two components, 110m ^{18}F and 15h ^{24}Na, the latter from pair production by the high energy γ-rays in the NaI crystal.

The activity of the blank Mylar foils (foils B in Fig. 1) was subtracted point-by-point from the activities in the Mylar catchers (foils C in Fig. 1). The resulting decay curves were analyzed by a 2-component least-squares computer program. The decay curve of the blank catcher is too complicated to warrant a simple least-squares analysis. The major impurity in the Mylar foils was shown by neutron activation analysis to be Sb.[9]

To eliminate the disturbance in the recoil results by the air between the target and the catchers, a small vacuum chamber was constructed for the irradiations. During a typical irradiation of 1 hr, the gas pressure inside the vacuum chamber rose from 0.04 Torr to 0.2 Torr. The experimental results done in air tended to have lower range values and higher forward-to-backward ratios than those done in vacuum, a consequence of the shorter range values of the backward recoils. Only the irradiations done in vacuum were used to measure the recoil properties. The cross section data are from all experiments. In all, two experiments in air and three in vacuum were performed.

The effect of secondary particles on the production of ^{18}F in the Al and U target assemblies was studied by use of the target arrangement of Fig. 1b. A sheet of uranium foil, 50 mg/cm^2 thick, was inserted between Al foils and stacked behind the Al target

assembly. The ^{24}Na and ^{18}F activities in the aluminum monitor foils (M_B and M_F) of the U target assembly and the Al and Mylar foils of the Al target assembly were counted after the irradiation. It was found that the ^{18}F activity in the aluminum target foil, corrected for recoil loss, was the same within counting statistics as those found in M_B and M_F of the U target assembly, whereas the ^{24}Na activity in the forward Al monitor, M_F, was 12% higher than in the Al target and 9% higher in the M_B monitor. The difference in ^{24}Na activities reflects the contribution of secondary neutrons from the U target to the ^{24}Na production. These results are consistent with previous measurements at 300 GeV.[10] From these results we conclude that the secondary particle production of ^{18}F from Al in ~50 mg/cm^2 U target assemblies is negligible and that the secondary neutron production in the Al target assemblies is $\lesssim$2% of the primary production. This result agrees with earlier work on secondary production of ^{24}Na from Al at 12 and 30 GeV.[11,12]

III. RESULTS

The cross section for production of ^{18}F from ^{27}Al at 400 GeV was found to be 5.9 ± 0.2 mb, based on an 8.0 mb cross section for the $^{27}Al(p,3pn)^{24}Na$ reaction.[13] This ^{18}F cross-section value is based on four measurements and a β^+ branching ratio of ^{18}F of 97% and is almost identical to that measured at lower energy (10-30 GeV) when corrected to the same ^{24}Na cross section.[14] The error quoted in the cross section is the standard

deviation of the mean; not included is the uncertainty of the counter efficiencies of about 8% and the error in the ^{24}Na cross section of about 7%.[13]

The thick-target recoil properties of ^{24}Na and ^{18}F are given in Table I. F and B are the fraction of the activity collected in the forward and backward catchers, respectively. W is the thickness of the Al foil in $\mu g/cm^2$. The recoil data were analyzed in accord with the two-step model in which the struck nucleus acquires a velocity $\underset{\sim}{v}$ with components $v_{\parallel}$ and $v_{\perp}$, relative to the proton beam, and the product formed after deexcitation has a speed V in the frame of the struck nucleus (moving frame). The quantities 2W(F+B) and W(F-B) are related to the fragment range in the moving frame, R, and the velocity ratio $\eta_{\parallel} = v_{\parallel}/V$ by the simplified expressions derived by Sugarman and coworkers[15]

$$2W(F+B) = R\left[1 + \eta_{\parallel}^{2}\ \frac{(N+1)^2}{4}\right] \tag{1}$$

$$W(F-B) = \eta_{\parallel} R\left(\frac{N+2}{3}\right) . \tag{2}$$

N is the constant in the range-velocity relationship $R = kV^N$. The N values for ^{24}Na and ^{18}F in Al are 1.38, 1.39, respectively, and those of k, 1.61 and 1.34, respectively, as calculated from the range-velocity table of Northcliffe and Schilling[16] corrected for the projection along the path length.[17] In the above analysis, it was assumed that the contribution from $\eta_{\perp}$ and b/a, the anistropy factor, were negligible. Included in Table I are the results at

lower energies reported by Poskanzer et al.[7] and Steinberg and Winsberg[8] analyzed in the same fashion. It was noted by Winsberg[18] that a thick-target $\eta_{\parallel}$ value differs from that of a thin target when V is not single-valued. The $\eta_{\parallel}$ values of Table I are really $\frac{\langle R\eta_{\parallel}\rangle}{\langle R\rangle}$ not $\langle\frac{v_{\parallel}}{V}\rangle$ and for the V distribution expected in this case[7] (see Discussion, Sec. IV) are ~25% smaller than the thin-target $\eta_{\parallel}$ values. Similarly, the V values of Table I are not $\langle V\rangle$ values, but rather $\langle V^N\rangle^{1/N}$, ~2.5% higher than $\langle V\rangle$. On the other hand, the $v_{\parallel}$ values of Table I are obtained from multiplying the $\eta_{\parallel}$ values by the V values, or $\frac{\langle R\eta_{\parallel}\rangle}{\langle R\rangle}\langle V^N\rangle^{1/N}$, only ~2% lower than the true $v_{\parallel}$ values. The E* values of Table I were obtained from the two-nucleon collision model of Turkevich[19] and used in the earlier analysis of Poskanzer et al.[7] and more recently by Scheidemann and Porile.[20] Specifically, $E^* = p_{\parallel}/(1+\frac{2}{T})^{\frac{1}{2}}$, where E* is the energy loss of the bombarding proton, $p_{\parallel}$ is the momentum of the struck nucleus (^{27}Al), and T is the kinetic energy of the bombarding proton. E* and T are given in the unit of the proton rest mass energy (m_oc^2) and $p_{\parallel}$ in the unit m_oc. This two-nucleon collision model will be examined in the next section.

IV. DISCUSSION

The values of FW, BW and $\eta_{\parallel}$ of Table I are plotted in Fig. 2 as a function of the bombarding energy, T_p, GeV. It is seen that from 3 GeV to 400 GeV, these quantities are well

represented by the following equations calculated from a weighted least squares analysis:

$$FW = (185\pm4) - (8.0\pm2.7) \log T_p, \quad (3)$$

$$BW = (65\pm2) + (5.3\pm1.2) \log T_p, \quad (4)$$

$$\eta_{\parallel} = (0.223\pm0.003) - (0.0243\pm0.0023) \log T_p, \quad (5)$$

where T_p is given in GeV and FW and BW in $\mu g/cm^2$ Al.
In each case, the error quoted is the standard unweighted error of the least squares value. If we denote by s the total center-of-mass-energy (considering nucleon-nucleon collision), in GeV^2, then $\eta_{\parallel}$ can be represented by

$$\eta_{\parallel} = (0.236\pm0.005) - (0.026\pm0.003) \log s. \quad (6)$$

From high energy proton-proton[21] and proton-nucleus bombardment[22] the average number of high-energy charged secondaries (mostly pions) per interaction was seen to increase with log s in the proton energy range 3-400 GeV from a value of ~2.5 at 3 GeV to ~9 at 400 GeV for p+p interactions and is ~1.5 times larger for p+Al interactions. Because this inelasticity may manifest itself in $p_{\parallel}$ for a given E* or in E* for a given $p_{\parallel}$, the two-step two-nucleon collision model was reexamined. Essentially what was done was an extension of the two-body kinematic analysis[23,24] used so successfully in the $(p,p\pi^+)$ reaction by Poskanzer et al.[25] on Al and by Remsberg[26] on Cu. If it is assumed that the primary p+Al interaction involves either projectile fragmentation or target nucleon fragmentation, then the rest mass of one of the particles has increased by the extra particle rest mass and the internal energy of that nucleon plus secondaries system. In

either case it is assumed that the struck nucleon deposits all of its energy and momentum in the nucleus (^{27}Al). Calling $\underline{w}$ the total rest mass of the fragmenting nucleon, with the unit m_o, we find that

$$p_{\parallel} = \frac{2(E+1)E^* \pm (\underline{w}^2-1)}{2p} \tag{7}$$

where p and E are the momentum and total energy of the bombarding proton, again with units $m_o c$ and $m_o c^2$, respectively. The <u>plus</u> sign refers to the case of projectile fragmentation and the <u>minus</u> sign to target nucleon fragmentation. When $\underline{w} = 1$, no fragmentation, the $p_{\parallel}$ - E* relation is that of a single elastic nucleon-nucleon collision given earlier. A comparison of the observed dependence of $p_{\parallel}$ on T_p with that calculated from the elastic nucleon-nucleon collision model, assuming a constant value of E* of 0.060, is given in Fig. 3. It is noted that in the T_p region of 3-400 $m_o c^2$ the deviation between the two curves is small and may be within experimental error. However, if the difference is attributed to $\underline{w} \neq 1$ for the projectile, then the values of $\langle \underline{w}^2 \rangle^{\frac{1}{2}}$ calculated at T_p values of 3, 30, and 400 for a constant E* value of 0.060 are ~1, ~1.2, and ~0.3. Only in the case of T_p equal to 30 does $\langle \underline{w}^2 \rangle^{\frac{1}{2}}$ exceed the mass needed for one pion production (1.15). Most probably, all of these values are unity within experimental error. This situation differs markedly from that expected for an average p + Al collision, ~14 pions, or from the value of $\langle \underline{w}^2 \rangle^{\frac{1}{2}}$ for the $^{27}Al(p,p\pi^+)$ reaction at 28 GeV of 3.65. The conclusion drawn from the ^{24}Na results is that there is no evidence

for projectile fragmentation in p+Al interactions producing ^{24}Na. Target nucleon fragmentation may also be ruled out on simple energetic grounds. The smallest value of w would be 1.15 corresponding to a minimum value of E* of 140 MeV, the rest mass of the pion. Since some 95% of E* would be in the form of excitation energy of ^{27}Al, the probability of ^{24}Na being an evaporation product would be negligibly small.

The values of R or V of Table I corresponding to the deexcitation step of the two-step model are seen to be essentially constant from 0.5 GeV to 400 GeV despite the change in $\eta_{\parallel}$ by more than a factor of 2 in this energy range. The average values of R and V are 464 ± 4 μg/cm^2 and 0.406 ± 0.003 (MeV/amu)$^{\frac{1}{2}}$, respectively, where each error is the standard deviation of the mean value ignoring individual errors. This constancy of R (or V) lends strong support to the two-step mechanism and implies that the deexcitation step is unaffected by the change in momentum transfer of the primary nucleon-nucleon collision. A similar conclusion was drawn by Winsberg et al.[27] in the case of ^{149}Tb produced by "deep spallation" from Au. What remains a "puzzle", however, is the magnitude of V, already discussed by Poskanzer et al.[7] The distribution of V expected from the evaporation[28] of particles from ^{27}Al excited to 60 MeV leads to an average V value some 65% of that observed. Poskanzer et al.[7] proposed that the extra contribution to V came from the momentum of the "hole" in the Fermi sea of nucleons left by the struck

nucleon. Since this explanation is kinematically unsound, it seems more likely that the extra contribution to V arises from high-energy complex particle emission resulting from pre-equilibrium deexcitation of highly excited nuclei. There is evidence for high-energy ^{24}Na recoils in the 10-20 MeV range from recent work of Poskanzer and coworkers.[29]

ACKNOWLEDGMENT

One of us (N.S.) gratefully acknowledges helpful discussions with Dr. J. B. Cumming of Brookhaven National Laboratory. We are grateful to the operating crew of Fermilab for their cooperation, and to R. A. Johns and Mrs. K. Wielgoz for counting and data processing.

REFERENCES

*Work supported in part by U. S. Energy Research and Development Administration.

1. R. Serber, Phys. Rev. 72, 1114 (1947).

2. N. Metropolis, R. Bivins, M. Storm, A. Turkevich, J. M. Miller, and G. Friedlander, Phys. Rev. 110, 185 (1958) and Phys. Rev. 110, 204 (1958).

3. K. Chen, Z. Fraenkel, G. Friedlander, J. R. Grover, J. M. Miller, and Y. Shimamoto, Phys. Rev. 166, 949 (1968).

4. J. Hudis, in Nuclear Chemistry, edited by L. Yaffe (Academic Press, New York, 1968), Vol. I, p. 169; also J. M. Alexander, ibid., p. 273.

5. N. M. Hintz, Phys. Rev. 87, 1042 (1952).

6. S.-C. Fung and I. Perlman, Phys. Rev. 86, 623 (1952).

7. A. M. Poskanzer, J. B. Cumming, and R. Wolfgang, Phys. Rev. 129, 374 (1963).

8. E. P. Steinberg and L. Winsberg, Phys. Rev. C10, 1925 (1974).

9. J. La Rosa, private communication.

10. S. K. Chang and N. Sugarman, Phys. Rev. C9, 1138 (1974).

11. Y. Y. Chu, E. M. Franz, and G. Friedlander, Nucl. Phys. B40, 428 (1972).

12. A. F. Stehney and E. P. Steinberg, Nucl. Inst. Meth. 59, 102 (1968).

13. S. B. Kaufman, M. W. Weisfield, B. D. Wilkins, D. H. Henderson, and E. P. Steinberg, Phys. Rev. C13, 253 (1976); also in press. J. B. Cumming, unpublished.

14. J. B. Cumming, Ann. Rev. Nucl. Sci. 13, 261 (1963).

15. N. Sugarman, H. Münzel, J. A. Panontin, K. Wielgoz, M. V. Ramaniah, G. Lange, and E. Lopez-Menchero, Phys. Rev. 143, 952 (1966).

16. L.C. Northcliffe and R. F. Schilling, Nuclear Data Tables Vol. 7, 233 (1970).

17. J. B. Cumming, private communication.

18. L. Winsberg and J. M. Alexander, in Nuclear Chemistry, edited by L. Yaffe (Academic Press, New York, 1968) Vol. I, p. 340.

19. A. Turkevich, as reported by N. T. Porile and N. Sugarman, Phys. Rev. 107, 1410 (1957).

20. Ø. Scheidemann and N. T. Porile, Phys. Rev. C, in press.

21. E. Albini, P. Capiluppi, G. Giacomelli, and A. M. Rossi, Il Nuovo Cimento 32A, 101 (1976).

22. J. R. Florian, M. Y. Lee, J. J. Lord, J. W. Martin, R. J. Wilkes, R. E. Gibbs, and L. D. Kirkpatrick, "Interaction of 300 GeV Protons with Tungsten and Chromium," Report of Cosmic Ray Laboratory, Department of Physics, University of Washington, Seattle, Wash., September, 1975.

23. L. Winsberg, Phys. Rev. 135, B1105 (1964).

24. J. B. Cumming, Phys. Rev. 137, B848 (1965).

25. A. M. Poskanzer, J. B. Cumming, and L. P. Remsberg, Phys. Rev. 168, 1331 (1968).

26. L. P. Remsberg, Phys. Rev. 138, B572 (1965).

27. L. Winsberg, M. W. Weisfield, and D. Henderson, Phys. Rev. C13, 279 (1976).

28. I. Dostrovsky, Z. Fraenkel, and G. Friedlander, Phys. Rev. 116 683 (1959).

29. Private communication from A. M. Poskanzer on fragments from 4.9-GeV proton bombardment of Al.

TABLE I. Recoil properties of ^{24}Na and ^{18}F from ^{27}Al bombarded with protons.

T_p GeV	2W(F+B) μg/cm^2 Al	W(F-B) μg/cm^2 Al	F/B	R μg/cm^2 Al	$\eta_{\parallel}$	V $\left(\frac{MeV}{amu}\right)^{\frac{1}{2}}$	$V_{\parallel}$ $\left(\frac{MeV}{amu}\right)^{\frac{1}{2}}$	E* MeV
400	488 ± 4	86 ± 4	2.09±0.10	470 ± 4	0.162±0.008	0.410±0.005	0.066±0.003	54± 2
300[a]	469 ± 7	85 ± 7	2.13±0.06	451 ± 7	0.167±0.014	0.397±0.006	0.066±0.006	54± 5
200[a]	482	88	2.14	464	0.166	0.406	0.067	55
28[b]	500 ± 4	95 ± 4	2.24±0.07	479 ± 4	0.178±0.008	0.415±0.003	0.074±0.003	59± 2
11.5[a]	475 ±10	100 ± 10	2.47±0.06	450 ± 9	0.199±0.020	0.397±0.008	0.079±0.008	61± 6
9[a]	496 ± 5	106 ± 5	2.51±0.05	469 ± 5	0.200±0.010	0.409±0.004	0.082±0.004	62± 3
6[a]	482 ±12	107 ± 12	2.59±0.06	454 ± 11	0.209±0.024	0.399±0.010	0.083±0.009	60± 7
3[a]	464 ±33	107 ± 33	2.72±0.08	434 ± 31	0.221±0.070	0.387±0.028	0.086±0.027	56±18
2.9[b]	505 ± 4	116 ± 4	2.68±0.09	474 ± 4	0.215±0.008	0.412±0.003	0.089±0.003	57± 2
2.25[b]	476 ± 8	108 ± 8	2.66±0.16	447 ± 8	0.214±0.016	0.395±0.007	0.085±0.006	52± 4
1.6[b]	507 ± 4	126 ± 4	3.00±0.15	469 ± 4	0.239±0.008	0.409±0.003	0.098±0.003	55± 2
1.0[b]	519 ±10	142 ± 10	3.44±0.25	470 ± 9	0.270±0.020	0.410±0.008	0.111±0.008	54± 4
0.8[b]	560 ± 4	170 ± 4	4.09±0.17	495 ± 4	0.305±0.007	0.425±0.003	0.130±0.003	59± 1
0.5[b]	559 ± 2	190 ± 2	5.27±0.24	474 ± 2	0.356±0.004	0.412±0.002	0.147±0.002	56± 1
400[c]	762 ±14	157 ± 14	2.40±0.18	724 ± 13	0.193±0.017	0.640±0.013	0.124±0.011	102± 9

a Reference 8.

b Reference 7.

c ^{18}F results. Although reproducible, these recoil results may be unreliable because of possible loss of ^{18}F from the Mylar catchers (early unreported work from Brookhaven National Laboratory and Lawrence Berkeley Laboratory and Reference 8).

FIGURE CAPTIONS

Fig. 1. Target assemblies for recoil and cross section measurements. M, Mylar foil (17 mg/cm^2); Al, aluminum foil (6.8 mg/cm^2); U, uranium foil (~50 mg/cm^2); G, guard foil; C, catcher foil; T, target foil; B, blank foil; M_B and M_F, monitor foils in the uranium target assembly.

Fig. 2. Dependence of FW, BW and $\eta_{\parallel}$ on proton bombarding energy, T_p.

Fig. 3. Variation of $p_{\parallel}$ with T_p. • measured values; ▪ calculated values from elastic nucleon-nucleon collision model.

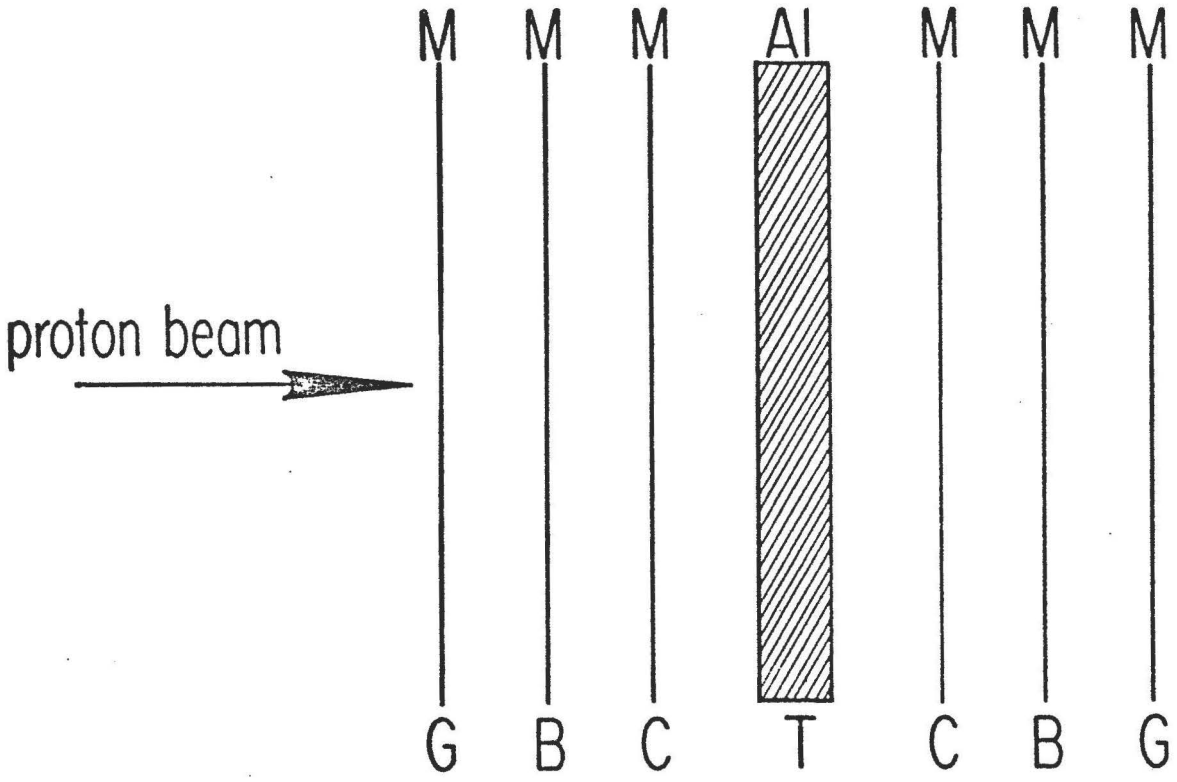

FIG. 1A. SIMPLE AL TARGET BOMBARDMENT ASSEMBLY.

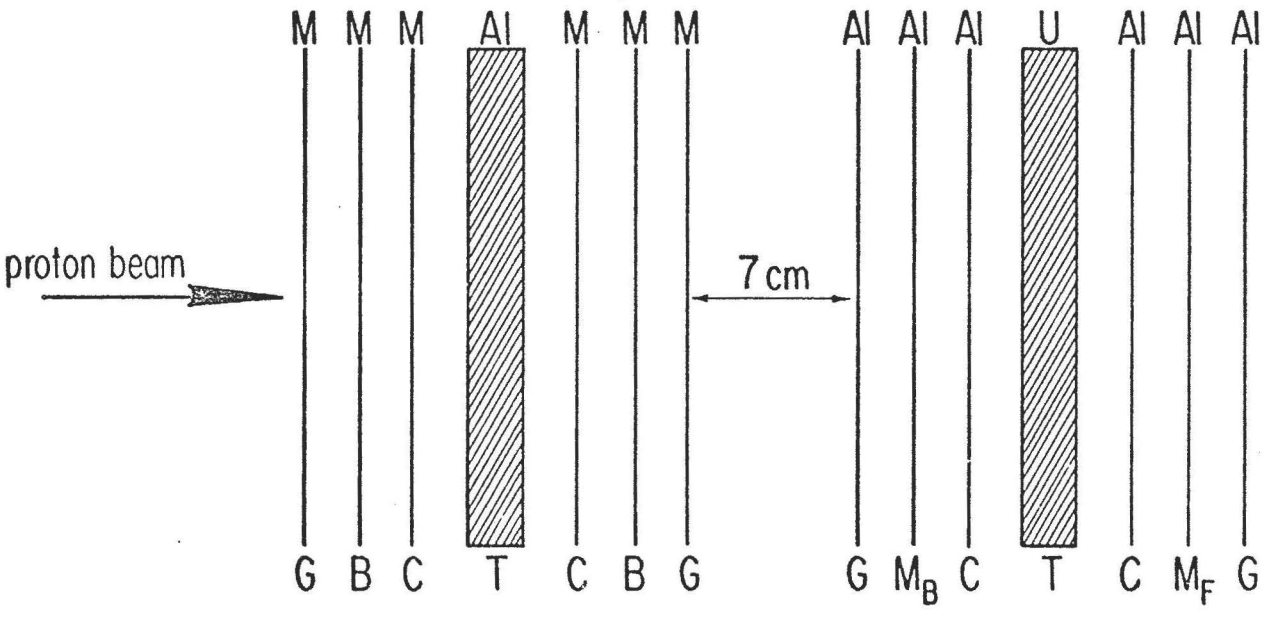

FIG. 1B. COMPLEX BOMBARDMENT ASSEMBLY FOR SECONDARY PARTICLE EFFECT.

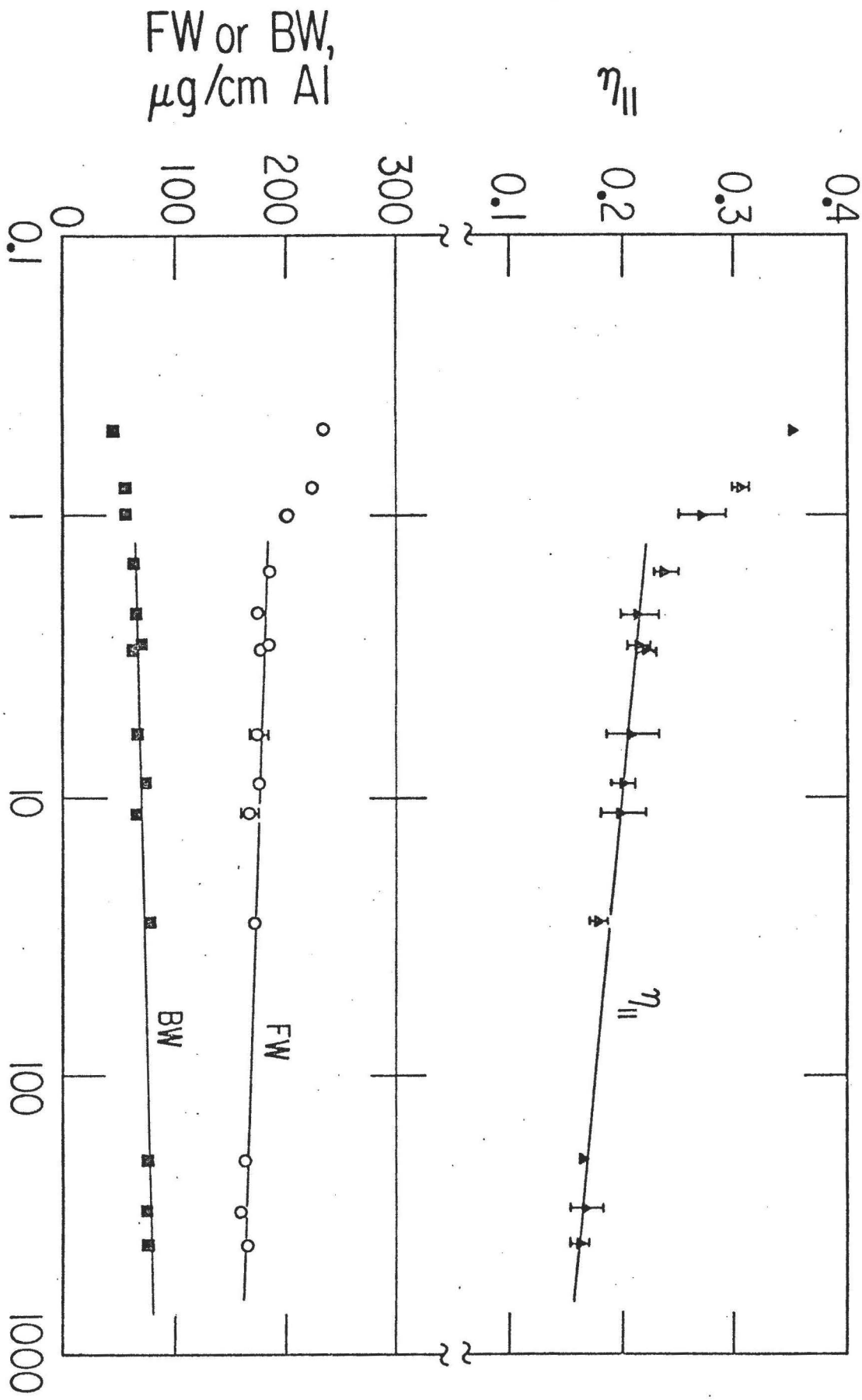
FW or BW,
μg/cm Al
0
100
200
300
0.1
0.2
0.3
0.4
$\eta_{\parallel}$
BW
FW
$\eta_{\parallel}$
0.1
1
10
100
1000
T_p, GeV

FIG. 2

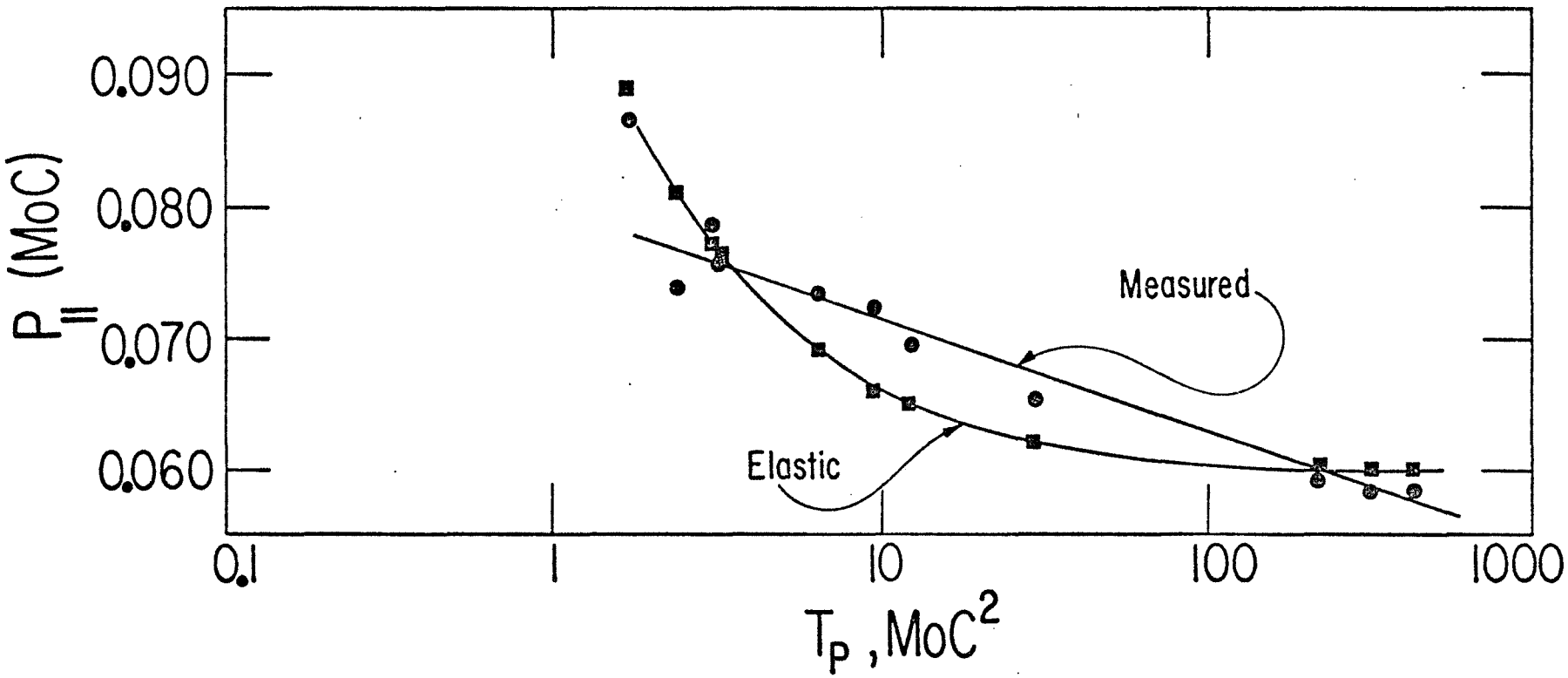
0.090
0.080
0.070
0.060
$P_{\parallel}$ (MoC)
0.1
1
10
100
1000
T_P , MoC^2
Measured
Elastic

FIG. 3